# Evaluation of Cardiac Sympathetic Innervation with Iodine-123-Metaiodobenzylguanidine Imaging in Silent Myocardial Ischemia

Shinro Matsuo, Masayuki Takahashi, Yasuyuki Nakamura and Masahiko Kinoshita
*First Department of Internal Medicine, Shiga University of Medical Science, Otsu, Japan*

An abnormality of the autonomic nervous system caused by diabetic neuropathy is one of the major causes of silent myocardial ischemia (SMI). This study evaluated quantitatively the association between clinically detectable SMI and myocardial $^{123}$I-metaiodobenzylguanidine (MIBG) uptake in patients with diabetes. **Methods:** Patients with SMI with diabetes, with SMI without diabetes, with angina pectoris with diabetes and normal control subjects participated in this study. Subjects underwent planar and SPECT imaging immediately and 3 hr after injection of [$^{123}$I]MIBG, and exercise thallium scintigraphy. MIBG was quantified based on the myocardial-to-mediastinal ratio (H/M) of [$^{123}$I]MIBG count, the inferior wall to anterior wall count ratio (I/A), the relative regional uptake (RRU), washout rate and corrected [$^{123}$I]MIBG defect score. **Results:** H/M ratio was significantly lower in diabetic SMI (2.1 ± 0.3) and nondiabetic SMI (2.3 ± 0.3) than in control subjects (2.6 ± 0.3). RRU was the lowest in inferior wall of the left ventricle in the normal group (78 ± 7). Compared with anterior segments, the uptake of [$^{123}$I]MIBG was lower in inferior and apex segments in normal subjects ($p < 0.05$). A significant difference was observed in RRU in the inferior segment of the distal left ventricle between SMI and angina groups ($p < 0.05$) among patients with diabetes mellitus. I/A ratio in the diabetic SMI group was the smallest ($p < 0.05$). However, no significant difference was observed in the corrected [$^{123}$I]MIBG defect score among all groups. **Conclusion:** The MIBG uptake was heterogeneous in normal subjects. Decreased MIBG uptake in the inferior wall may be an important sign of cardiac sympathetic dysfunction, suggesting that the abnormalities in cardiac nervous system play an important role in the mechanism of silent myocardial ischemia.

**Key Words:** silent myocardial ischemia; sympathetic innervation; metaiodobenzylguanidine; scintigraphy; diabetes

**J Nucl Med 1996; 37:712–717**

Silent myocardial ischemia (SMI) implies no subjective pain sensation in the presence of positive signs of myocardial ischemia. As shown in previous studies, the afferent fibers running through the cardiac sympathetic nerves form a pathway essential for transmission of cardiac pain (*1,2*). It was reported that the incidence of silent myocardial infarction in diabetic patients is higher than that in nondiabetic subjects (*3*). Although the pathophysiological reason for this is still unclear, an abnormality of the autonomic nervous system resulting from diabetic neuropathy has been suggested to be the major cause (*4*). A previous histological study revealed lesions typical of autonomic neuropathy of afferent sensory nerve in the heart in patients with diabetes and silent myocardial infarction (*5*). However, little is known regarding the pathophysiology of SMI due to the lack of techniques for direct assessment of the damage in sympathetic neurons in the living heart.

Metaiodobenzylguanidine (MIBG), an analog of guanethidine, is taken up and stored similarly to norepinephrine. It is taken up by sympathetic efferent nerve terminals, which are most abundant in left ventricle. Iodine-123-labeled MIBG is used for imaging and functional assessment of sympathetic innervation of the heart (*6*). Distribution of MIBG uptake is heterogeneous in normal subjects, with a relatively low uptake in inferior and apical regions (*6,7*). Abnormalities in myocardial [$^{123}$I]MIBG uptake were reported in patients with coronary artery disease (*8,9*), diabetes (*10*), cardiomyopathies (*11*), long QT syndrome (*12*) and generalized autonomic neuropathy (*6*). These abnormal profiles of [$^{123}$I]MIBG uptake reflect injury to, and functional alterations in, adrenergic fibers into the heart.

The aim of this study was to quantitatively evaluate the association between clinically detectable silent myocardial ischemia and myocardial [$^{123}$I]MIBG uptake in patients with diabetes.

## MATERIALS AND METHODS

### Patient Population

Thirty-six patients, admitted to our university hospital for suspected coronary artery disease (CAD), were enrolled in this study. Based on the results of treadmill testing and the presence of diabetes mellitus, patients were divided into three groups: (a) diabetic angina group, (b) diabetic SMI group and (c) nondiabetic SMI group. SMI was defined by positive myocardial ischemia as evidenced by reversible perfusion defect on exercise $^{201}$Tl scintigraphy in conjunction with ST segment depression without chest pain (*4*). All patients had significant angiographic coronary artery disease (>75% in ≥1 major coronary artery by AHA definition). Patients were excluded from the study if they had myocardial infarction, reduced ejection fraction (≤ 45%), thyroid disease or malignant disease, were unwilling to participate or were receiving medications that could have interfered with the uptake of [$^{123}$I]MIBG (beta-blockers or antidepressants). At enrollment, complete medical histories were taken and physical examinations were performed in all patients. The control group consisted of 22 normal subjects without ischemic heart disease or diabetes mellitus. The study was approved by our institutional review board and informed consent was obtained from all subjects before they underwent any of the investigations.

### Exercise Treadmill Test

Maximal exercise treadmill testing was performed according to the Bruce (*13*) protocol. The 12-channel electrocardiogram (ECG) was monitored continuously and blood pressure was recorded at baseline, at the end of each exercise stage, at the onset of ischemia and at peak exercise. The exercise ECG response was considered ischemic when horizontal or down-sloping ST-segment was de-

Received Jan. 27, 1995; revision accepted Oct. 8, 1995.
For correspondence or reprints contact: Shinro Matsuo, MD, First Department of Internal Medicine, Shiga University of Medical Science, Seta, Otsu Shiga 520-21, Japan.

pressed more than 0.1 mV from baseline, or when up-sloping depression ≥0.15 mV was observed 60 msec after the J point.

### Thallium-201 SPECT

Each subject performed treadmill exercise according to the Bruce protocol (*13*), with continuous monitoring of heart rate, 12-lead ECG, blood pressure and symptoms. At peak exercise, approximately 111 MBq of $^{201}$Tl was injected intravenously and exercise was continued for an additional 60 sec. Image acquisition was initiated 6 min after the injection of thallium using a low-energy, general-purpose gamma camera (GCA-901, Toshiba Co. Ltd., Tokyo, Japan) with a 20% window. Thirty-two projections (40 sec) were obtained, spanning from a 45° right anterior oblique to a 45° left posterior oblique view. Redistribution imaging was obtained 3 hr after initial imaging. From the raw scintigraphic data, tomographic images (slices 6mm thick) were reconstructed along the short, horizontal and vertical long axis of the left ventricle using the manufacturer's software (GMS-5504, Toshiba Co. Ltd, Tokyo, Japan) by means of a back-projection algorithm with filtering and without attenuation correction.

### Iodine-123-MIBG Scintigraphy

Iodine-123-MIBG at a dose of 111 MBq was injected slowly through the antecubital venous cannula and flushed with 10 ml saline at rest after a 3-hr fast. The planar and SPECT views were obtained approximately 15 min after injection, using the same protocol as the $^{201}$Tl study. Delayed imaging was obtained 3 hr after initial imaging. During the period between the initial and delayed scans, the subjects continued fasting.

### Data Analysis

Coronary angiography was performed in all patients through the femoral artery within the 2-wk period of radionuclide studies. Multiple views of both coronary arteries were obtained. All angiograms were evaluated visually by two independent observers.

Two-dimensional echocardiographic studies (SSH-160A Toshiba, Tokyo, Japan) were performed within 1 wk of the radionuclide studies in all patients, and included long-axis, short-axis and apical four-chamber views. The left ventricular mass was measured by an M-mode echocardiographic quantification using the Penn convention (*14*).

Cardiac uptake was quantified in planar anterior views at 15 min and 3 hr after injection of MIBG. As shown in Figure 1, the regions of interest on planar imaging were set at the mediastinum (M) and the heart (H) to quantify cardiac MIBG-uptake in terms of the H/M activity ratio (*11,15*). The clearance rate from the myocardium (washout rate) was calculated as follows: (initial myocardial MIBG uptake − delayed myocardial MIBG uptake)/initial myocardial MIBG uptake × 100. In SPECT imaging, the intensity of each image was normalized to the highest pixel value in that image. The left ventricular myocardium was divided into 9 segments (distal and basal anterior, septal, inferior, lateral and apical segments) as shown in Figure 2.

Thallium-201 and [$^{123}$I]MIBG scintigrams were read by two independent experts for the presence of any abnormalities, without prior knowledge of the clinical, exercise or angiographic results. A four-point scoring system by visual interpretation (3 = absence of detectable tracer in a segment; 2 = severe reduction of radioisotope uptake; 1 = moderate; 0 = normal radioisotope uptake) for 324 segments of left ventricular myocardium was used as a defect score for the stress $^{201}$Tl perfusion and [$^{123}$I]MIBG uptake. In $^{201}$Tl image, a reversible perfusion defect was determined by one or more grade improvements of uptake on the 3-hr image compared with the early image.

A square region of interest of 5 × 5 pixels was placed over the center of each of the nine segments, and regional uptake was determined for each segment as the mean count per pixel within the corresponding region of interest as in Figure 2. Moreover, the relative regional uptake (RRU %) was determined for each segment as the ratio of its regional uptake to the maximum regional uptake among the short-axis slices (*16*). The inferior wall to anterior wall count ratio (I/A) was calculated from the mean counts

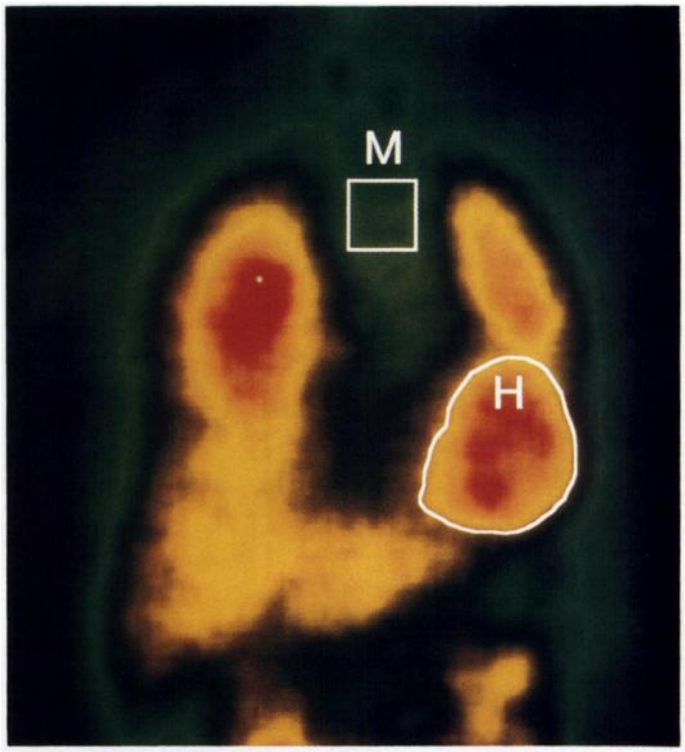


**FIGURE 1.** Regions of interest on planar imaging with [$^{123}$I]MIBG were set as the mediastinum (M) and heart (H). Cardiac MIBG uptake was quantified in terms of the H/M activity ratio.

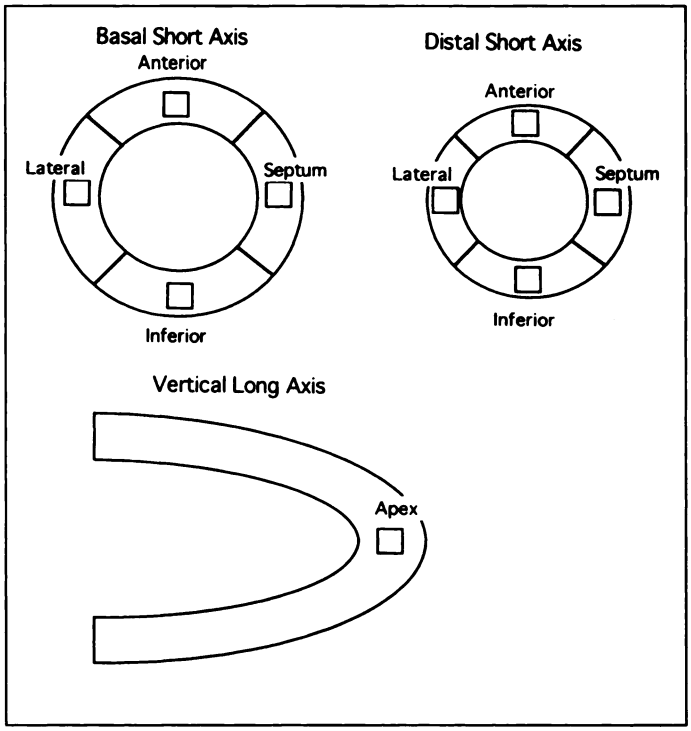


**FIGURE 2.** Two short-axis images at the basal and distal levels and a vertical long-axis image at the mid-left ventricle were selected for quantitative analysis. Regions of interest, 5 × 5 pixels in size, were determined over the myocardium as displayed.

**TABLE 1**
Baseline Clinical and Procedural Variables

| | Diabetic SMI (n = 14) | Diabetic angina (n = 14) | Nondiabetic SMI (n = 8) |
|---|---|---|---|
| Clinical data | | | |
| Age (yr) | 63 ± 9 | 61 ± 9 | 58 ± 6.0 |
| Gender (M/F) | 11/3 | 7/7 | 7/1 |
| Diabetes | | | |
| Hbalc (%) | 8.9 ± 1.3 | 8.2 ± 1.2 | |
| Duration of diabetes (yr) | 7.7 ± 3* | 5.0 ± 2* | |
| Neuropathy† | 3 | 2 | 0 |
| Nephropathy‡ | 2 | 2 | 0 |
| Cardiac parameter | | | |
| LVEF | 68 ± 8 | 65 ± 6 | 71 ± 6 |
| CTR (%) | 49 ± 2 | 47 ± 2 | 48 ± 3 |
| S/M/T | 9/4/1 | 9/4/1 | 7/1/0 |
| LVM (g/m$^2$) | 105 ± 4 | 104 ± 3 | 105 ± 5 |

mean value ± s.d.
*$p < 0.05$ between SMI and angina.
†Absence of ankle-jerk deep tendon reflex.
‡Serum creatinine ≥ 1.5 mg/dl.
LVM = left ventricular mass.
CTR = cardiothoracic ratio; LVEF = left ventricular ejection fraction by echocardiography; SMI = silent myocardial ischemia; DM = diabetes mellitus; Hbalc = acetylated hemoglobin; S/M/T = single-/multi-/triple-vessel disease.

in each segment. To account for abnormal [$^{123}$I]MIBG uptake on the basis of perfusion abnormalities, a corrected [$^{123}$I]MIBG defect score was calculated by subtracting $^{201}$Tl defect score in the delayed image from [$^{123}$I]MIBG defect score on a segment-by-segment basis and then averaged for nine segments.

### Statistical Analysis

All values are presented as mean values ± s.d. Scheffe's F test for multiple comparisons was applied to detect significant differences as defined by ANOVA. Student's t-test was used for comparison of paired data and $p < 0.05$ was considered significant.

## RESULTS

Clinical characteristic, diabetes states and cardiac parameters of CAD are summarized in Table 1. The duration of diabetes mellitus was 0.5–14 yr in diabetes groups. Twenty patients were treated with oral hypoglycemic agents, and 4 with insulin. The duration of diabetes was longer in the SMI than in the angina group ($p < 0.05$). There were no significant differences in the incidence of neuropathy or nephropathy between the two groups.

The degree of CAD, and prevalence of single-, double- and triple-vessel disease were similar among the three patient groups. No significant difference was observed in the incidence of right coronary disease, left anterior descending artery disease or left circumflex artery disease among the three patient groups. In both the diabetic SMI group and diabetic angina group, nine patients had single-vessel disease, four had multi-vessel disease and one had triple-vessel disease. In the nondiabetic SMI group, seven patients had single-vessel disease, one had multi-vessel disease and no patients had triple-vessel disease.

Exercise treadmill test parameters for the three patient groups are summarized in Table 2. No difference was observed in clinical characteristics, exercise performance in terms of exercise duration or pressure rate products (heart rate × systolic blood pressure) at rest or at peak exercise. There was no notable difference in the magnitude of maximum ST-segment depression among the three patient groups.

**TABLE 2**
Results of Exercise Treadmill Testing

| | Diabetic SMI (n = 14) | Diabetic angina (n = 14) | Nondiabetic SMI (n = 8) |
|---|---|---|---|
| Treadmill test duration (sec) | 480 ± 67 | 421 ± 59 | 462 ± 34 |
| Pressure rate product | | | |
| Rest (×10$^2$) | 86 ± 14 | 82 ± 10 | 90 ± 90 |
| Peak (×10$^2$) | 247 ± 37 | 249 ± 49 | 259 ± 22 |
| End point | | | |
| Chest pain | 0 | 14 | 0 |
| Dyspnea | 8 | 0 | 3 |
| Leg fatigue | 6 | 0 | 5 |
| Max ST segment depression (mV) | −0.19 ± 0.1 | −0.20 ± 0.09 | −0.20 ± 0.08 |

mean value ± s.d.
Pressure rate products = heart rate × systolic blood pressure. SMI = silent myocardial ischemia.

Two-dimensional echocardiography identified no akinetic or dyskinetic lesions of the left ventricle in a subject. No significant differences were observed in left ventricular mass among the three groups.

The incidence of segments with redistribution of exercise $^{201}$Tl is shown in Table 3. In each vascular territory, no significant difference was observed between diabetic patients with or without silent ischemia.

Cardiac MIBG-uptake as measured by the heart-to-mediastinum ratio (H/M) and the washout rate is shown in Figure 3. There was a significant difference in the H/M between diabetic SMI and normal groups (2.1 ± 0.3 versus 2.6 ± 0.3, $p < 0.01$, Scheffe's test) but not between diabetic SMI and angina groups (2.1 ± 0.3 versus 2.3 ± 0.3, NS), although there was a slight decrease in H/M in diabetic SMI group. There was a significant difference in the H/M between nondiabetic SMI and normal groups (2.3 ± 0.3 versus 2.6 ± 0.3, $p < 0.01$). An increased washout rate of [$^{123}$I]MIBG was observed in the SMI group when compared with the normal group (34 ± 4 versus 28 ± 3, $p < 0.01$). No statistically significant difference was observed in washout rate between the diabetic SMI and diabetic angina groups (34 ± 4 versus 31 ± 3, NS).

Table 4 shows [$^{123}$I]MIBG uptake in all patient groups. The MIBG uptake was heterogeneous in the normal group, with the lowest uptake in the inferior wall of the left ventricle (78 ± 7). When compared with the basal anterior segments, the basal inferior and apex had lower uptake of [$^{123}$I]MIBG ($p < 0.05$). The distal inferior segment had lower uptake than the distal anterior segment (78 ± 7 versus 90 ± 3, $p < 0.05$). In SPECT images of diabetic SMI, the distal inferior RRU had the least uptake (56 ± 9), and the anterior segment at the basal level had

**TABLE 3**
Regional Perfusion Abnormalities Identified by Exercise Thallium-201 in Patients with SMI

| | Diabetic SMI | Diabetic angina | Nondiabetic SMI |
|---|---|---|---|
| Anterior or septal | 7 (29%) | 8 (33%) | 4 (45%) |
| Inferior | 8 (33%) | 8 (33%) | 3 (33%) |
| Lateral | 4 (17%) | 4 (17%) | 1 (11%) |
| Apex | 5 (21%) | 4 (17%) | 1 (11%) |

Numbers in parentheses represent percentages of segments.
SMI = silent myocardial ischemia.

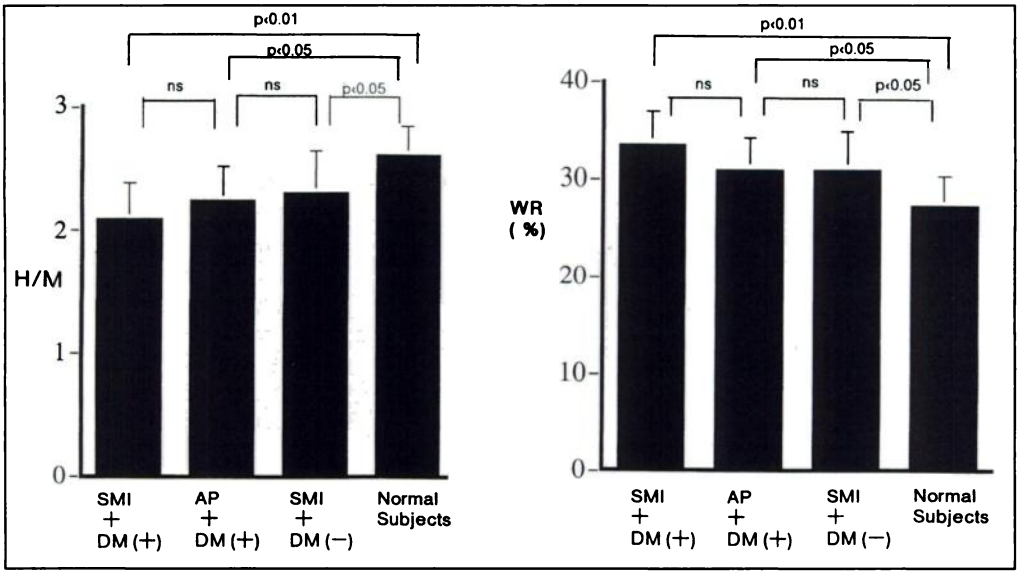


**FIGURE 3.** MIBG H/M in delayed imaging and washout rate in the control, and in diabetic SMI, nondiabetic SMI and diabetic angina groups. Values are expressed as means ± s.d. NS = not significant; H/M = the myocardial-to-mediastinal ratio; WR = washout rate; SMI = silent myocardial ischemia; AP = angina pectoris; DM = diabetes mellitus.

the greatest (86 ± 4). When compared with the basal anterior segments, the basal inferior and apex had lower uptake of [$^{123}$I]MIBG ($p < 0.01$). And the distal inferior segment had lower uptake than the distal anterior (55 ± 9 versus 86 ± 3, $p < 0.05$). On the other hand, the inferior-to-anterior wall count ratio (I/A) in diabetic SMI group was the lowest among all groups ($p < 0.05$). The most reduced [$^{123}$I]MIBG uptake in the inferior segment was observed in the diabetic SMI group, as shown clearly in Figure 4, representing a typical patient with SMI. Iodine-123-MIBG provided high-contrast tomograms of the left ventricular myocardium (Fig. 4).

There were no significant differences in the corrected [$^{123}$I]MIBG defect score among the three groups (diabetic SMI 0.47 ± 0.20, diabetic angina 0.42 ± 0.16, nondiabetic SMI group 0.42 ± 0.20).

**TABLE 4**
Relative Regional Uptake and Other Variables of MIBG for Each Segment at Basal and Distal Ventricle and Apex in All Four Groups

| | Diabetic SMI (n = 14) | Diabetic angina (n = 14) | Nondiabetic SMI (n = 8) | Control (n = 21) |
|---|---|---|---|---|
| Basal | | | | |
| Anterior | 86 ± 4 | 91 ± 4 | 90 ± 3 | 90 ± 3† |
| Lateral | 82 ± 6 | 84 ± 5 | 86 ± 3 | 91 ± 4 |
| Inferior | 57 ± 8 | 66 ± 11 | 63 ± 1 | 78 ± 7† |
| Septal | 76 ± 13 | 80 ± 8 | 80 ± 3 | 86 ± 4 |
| Distal | | | | |
| Anterior | 86 ± 3 | 88 ± 2 | 89 ± 3 | 90 ± 3† |
| Lateral | 81 ± 5 | 82 ± 8 | 86 ± 4 | 90 ± 4 |
| Inferior | 55 ± 9* | 66 ± 5* | 64 ± 2 | 78 ± 7† |
| Septal | 79 ± 8 | 83 ± 9 | 80 ± 3 | 88 ± 3 |
| Apex | 74 ± 9 | 78 ± 7 | 78 ± 3 | 83 ± 4‡ |
| I/A (basal) | 0.66 ± 0.09 | 0.73 ± 0.1 | 0.71 ± 0.2 | 0.86 ± 0.08 |
| I/A (distal) | 0.64 ± 0.1 | 0.75 ± 0.1 | 0.70 ± 0.2 | 0.87 ± 0.08 |
| Washout rate | 34 ± 4 | 31 ± 3 | 31 ± 4 | 28 ± 3 |
| H/M | 2.1 ± 0.3 | 2.3 ± 0.3 | 2.3 ± 0.3 | 2.6 ± 0.3 |

mean value ± s.d.
*$p < 0.05$ between diabetic SMI and diabetic angina.
†Significant difference between anterior and inferior segment.
‡Significant difference between anterior and apex.
SMI = silent myocardial ischemia; I/A = inferior-to-anterior wall count ratio.

## DISCUSSION

### Mechanisms of Silent Ischemia

Several explanations have been proposed for the mechanism(s) of silent ischemia, including increased threshold of pain receptor against noxious stimuli, neuronal or axon degeneration of C or Aδ nerve fibers and augmented pain-inhibitory system (*17*). The incidence of SMI was reported to be high in patients with diabetes mellitus, which was explained by autonomic neuropathy as one of major complications of diabetes (*5*). The afferent fibers running through the cardiac sympathetic and parasympathetic nerves form a pathway essential for transmission of cardiac pain (*2*). From the heart, afferent nerve fibers run to the dorsal root of the spinal cord via the upper five thoracic sympathetic ganglia, white rami communicantes, gray rami, and upper dorsal thoracic roots (*1*). Diabetic neuropathy was suggested to interfere with afferent cardiac nerves leading to loss of noxious perception as well as diabetes-induced neuropathy of efferent fibers. However, few studies have examined the mechanism(s) of silent myocardial ischemia and sought to identify the site(s) of autonomic nervous system dysfunction.

Faerman et al. explored autonomic nerve fibers at autopsy (*5*). Using histological techniques, they searched for lesions in the sympathetic and parasympathetic nerve fibers that conduct pain within the infarcted myocardium of diabetic and nondiabetic patients who died as a result of silent myocardial infarction. They found morphologic alterations of the sympathetic and parasympathetic nerves, such as beaded thickening within

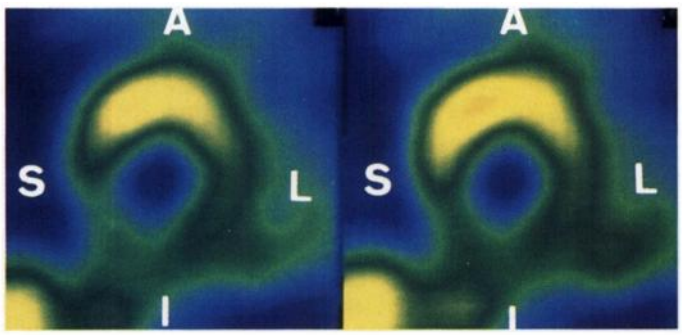


**FIGURE 4.** Representative short-axis [$^{123}$I]MIBG images in a patient (67-year-old man) with silent myocardial ischemia. Reduced [$^{123}$I]MIBG accumulation in the inferior segment of the distal left ventricle was observed. A = anterior; S = septum; I = inferior; L = lateral.

the nerves, spindle-shaped nerve fibers, fragmentation of nerve fibers and a decrease in the actual number of neurons. In five diabetic patients with painful infarction and five diabetic patients without infarction who had died from noncardiac causes, no such neuropathic alterations were observed. Thus, diabetic neuropathy may involve cardiac afferent sensory fibers, which would interfere with the transmission of pain.

### MIBG as a Tracer for Neuronal Injury

The synthetic compound MIBG has many cellular transport properties similar to those of norepinephrine, including neuron-specific uptake-1 (*18*), granular storage and secretion in response to acetylcholine. Defects in [$^{123}$I]MIBG uptake on delayed imaging reflect injury to, and functional alterations in, adrenergic fibers innervating the heart. This notion is now supported by a growing number of observations which include a substantial reduction in [$^{123}$I]MIBG uptake after transmitter depletion by 6-hydroxydopamine, and abnormalities in [$^{123}$I]MIBG uptake in patients with cardiomyopathies (*11*), long QT syndrome (*12*) and after myocardial infarction (*9*).

In agreement with previous reports (*9*), the imaging defects in the [$^{123}$I]MIBG scans were always more extensive than those in $^{201}$Tl scans, thus indicating that areas of sympathetic denervation were not limited to the necrotic zones, but also extended apically to noninfarcted myocardium. Previous animal studies (*19–21*) have shown that myocardial ischemia can stimulate both sympathetic and parasympathetic cardiac afferents. Muntz et al. (*22*) observed a greater reduction in the percent volume of nerve terminals and in the biochemically measured levels of tissue catecholamines after 3 hr of ischemia, suggesting that a local release of norepinephrine had occurred. Therefore, a patchy distribution of nerve terminals was observed, which raised the possibility that sympathetic imbalance may occur in regions of severe ischemia. The repeated episodes of ischemia in the myocardium may cause functional changes in nerve fibers (*23,24*) and the sympathetic nerves may be more susceptible than cardiac muscle to permanent ischemic damage because of the consistent occurrence of denervation within nontransmural lesions, with preserved viability of myocytes.

MIBG was considered to be taken up by sympathetic efferent nerve terminals. It is unclear whether it is also taken up by sympathetic afferents, since the sensory neurotransmitter has not yet been identified. However, it is possible that [$^{123}$I]MIBG uptake indirectly reflects the innervation of afferent nerves which run through with sympathetic efferent nerves.

The heterogeneity of MIBG distribution was reported in normal subjects. Tsuchimochi et al. (*25*) demonstrated in elderly normal individuals that [$^{123}$I]MIBG uptake was the lowest in the inferior wall of the left ventricle, in accordance with the results of our study. In contrast, Sisson et al. showed reduced uptake of [$^{123}$I]MIBG at the apex (*6*). Gill et al. studied normal subjects and showed a reduction of [$^{123}$I]MIBG uptake in the inferior and septal region (*7*). Our findings (Table 4) are similar to those of previous reports, and indicate that sympathetic nerve function of the inferior wall and apex may be decreased in normal subjects.

### Neuronal Injury in Diabetic Patients with SMI

Our study demonstrated that patients with silent ischemia showed decreased global [$^{123}$I]MIBG uptake and increased washout rate, compared to those in normal controls. However, these values were not significantly different from those in the diabetic angina group. Planar imaging of the H/M ratio is a simple method which allows comparison of inter-individual and inter-institutional results, by correcting for differences in body geometry and attenuation between individual subjects. The decreased H/M ratio observed in this study indicates that ischemia with diabetes causes neuronal injury and reduces innervation. Silent myocardial ischemia could not be detected by the value of H/M as an index of global neuropathy of myocardium, since there was no significant difference between the silent ischemia and angina groups in diabetic patients.

Regarding the regional differences, the RRU of the silent ischemia group and the angina group revealed a significant decrease in [$^{123}$I]MIBG uptake in the inferior wall, compared to the anterior wall. In SPECT images of silent ischemia with diabetes, the inferior RRU showed the least uptake, and anterior segments at the basal level had the greatest uptake. A significant difference between the silent ischemia group and the angina group was observed in the inferior segment of the left ventricle. Thus, there appears to be some degree of heterogeneity in [$^{123}$I]MIBG uptake in the hearts of patients with silent ischemia. Our results, shown in Tables 1 and 4, suggest that cardiac neuronal injury starts in the most distal inferior sites of sympathetic nerve fibers and progresses with time. While the regional changes in the cardiac adrenergic nervous system were complex, they characteristically showed primary involvement of the inferior segment of the left ventricle, which might be more sensitive than other regions.

In a recent study with diabetic patients (*10*), low uptake of [$^{123}$I]MIBG was observed in the inferior wall, with normal uptake of $^{201}$Tl in diabetics with nonautonomic neuropathy. Our study clearly demonstrated the abnormalities in cardiac autonomic dysfunction in patients with diabetes mellitus, especially those with silent myocardial ischemia. Involvement of the inferior wall in cardiac neuropathy, including the afferent neuronal fibers, may be an important diagnostic sign in silent myocardial ischemia. These new observations provide improved understanding of the pathogenesis of this disease. The decrease in [$^{123}$I]MIBG uptake suggests a total reduction in the number of sympathetic nerve terminals or the amount of damage to the affected sympathetic neurons in the heart, as demonstrated histologically by Faerman et al. (*5*).

The mechanism of decreased inferior uptake of [$^{123}$I]MIBG could be explained by the experimental observations that the inferior wall of the left ventricle has predominantly parasympathetic innervation, and that the anterior wall shows primarily sympathetic innervation. Our findings provide evidence of greatly reduced [$^{123}$I]MIBG uptake of the inferior wall in silent myocardial ischemia, suggesting that abnormalities in cardiac sympathetic denervation may be the basis for the ischemia being asymptomatic. The reduced inferior uptake was directly correlated with the severity of sympathetic dysfunction and became prominent with progression of dysfunction.

Iodine-123-MIBG photons have more energy than those from thallium. Thus, reduced inferior uptake cannot be explained by attenuation. In this study the camera was rotated through 180° to collect data. As shown previously (*26*), this rotation is more sensitive for detecting inferior and lateral abnormalities than a rotation of 360°. It is unlikely that regional differences in uptake resulted from methodological problems during data acquisition, since [$^{123}$I]MIBG uptake was calculated per unit area to exclude differences in the sizes of the regions and the wall thicknesses being assessed.

We should note that PET after intravenous injection of $^{11}$C-hydroxyephedrine (*27*) is more accurate than SPECT of [$^{123}$I]MIBG, with respect to quantification. However, there are relatively few PET facilities available, and the cost-benefit ratio is unclear. To our knowledge, there have been no reports of PET studies of silent myocardial ischemia.

Since the main limitation of the present study was the small

number of patients investigated, our general conclusions remain speculative.

### Clinical Implications of SMI in Diabetic Patients

The absence of angina does not necessarily confer a benign prognosis in patients with angiographically-proven coronary artery disease. It has been reported that the severity of angina is not related to the severity of coronary artery disease or to long-term prognosis (*28*). Furthermore, in patients with advanced coronary artery lesions, episodes of acute repetitive silent ischemia precipitate ventricular fibrillation, confirming the role of silent ischemia in the genesis of life-threatening ventricular arrhythmia (*29,30*).

## CONCLUSIONS

The MIBG uptake was heterogeneous in normal subjects. Decreased MIBG uptake in the inferior wall may be a diagnostic sign of cardiac sympathetic dysfunction in silent myocardial ischemia in diabetes suggesting that abnormalities in the cardiac nervous system play an important role in the mechanism of silent myocardial ischemia. Iodine-123-MIBG may provide a new approach for understanding and characterizing SMI, although the precise clinical importance of [$^{123}$I]MIBG scintigraphy in the diagnosis of silent ischemia must be determined by the outcome of further prognostic studies.


## ACKNOWLEDGMENTS

The authors thank Drs. Shintaro Yoshida and Tohru Inoue for their expert technical assistance.


## REFERENCES


1. White JC. Cardiac pain, anatomical pathways and physiologic mechanisms. *Circulation* 1959;16:644–655.
2. Takahashi M, Yokota T. Convergence of cardiac and cutaneous afferents onto neurons in the dorsal horn of the spinal cord in the cat. *Neurosci Lett* 1983;38:251–256.
3. Nesto RW, Watson FS, Kowalchuk GJ, et al. Silent myocardial ischemia and infarction in diabetics with peripheral vascular disease: assessment by dipyridamole thallium-201 scintigraphy. *Am Heart J* 1990;120:1073–1077.
4. Langer A, Freeman MR, Josse RG, Steiner G, Armstrong PW. Detection of silent myocardial ischemia in diabetes mellitus. *Am J Cardiol* 1991;67:1073–1078.
5. Faerman I, Faccio E, Milei J, et al. Autonomic neuropathy and painless myocardial infarction in diabetic patients: histologic evidence of their relationships. *Diabetes* 1977;26:1146–1158.
6. Sisson JC, Shapiro B, Meyers S, et al. Metaiodobenzylguanidine to map scintigraphically the adrenergic nervous system in man. *J Nucl Med* 1987;28:1625–1636.
7. Gill JS, Hunter GJ, Gane G, Camm AJ. Heterogeneity of the human myocardial sympathetic innervation: in vivo demonstration by iodine-123-labeled metaiodobenzylguanidine scintigraphy. *Am Heart J* 1993;126:390–398.
8. Shakespeare CF, Page CJ, Doherty MJ, et al. Regional sympathetic innervation of the heart by means of metaiodobenzylguanidine imaging in silent ischemia. *Am Heart J* 1993;125:1614–1622.
9. McGhie AI, Corbett JR, Akers MS, et al. Regional cardiac adrenergic function using $^{123}$I-metaiodobenzylguanidine tomographic imaging after acute myocardial infarction. *Am J Cardiol* 1991;67(4):236–242.
10. Nagamachi S, Hoshi H, Ohnishi T, et al. Iodine-123-MIBG myocardial scintigraphy in diabetic patients: association with autonomic neuropathy. *Jpn J Nucl Med* 1994;31: 1059–1069.
11. Nakajima K, Bunko H, Taki J, Shimizu M, Muramori A, Hisada K. Quantitative analysis if $^{123}$I-metaiodobenzylguanidine (MIBG) uptake in hypertrophic cardiomyopathy. *Am Heart J* 1990;119:1329–1337.
12. Gohl K, Feistel H, Weikl A, Bachmann K, Wolf F. Congenital myocardial sympathetic dysinnervation (CMSD)—a structural defect of idiopathic long QT syndrome. *Pace Pacing Clin Electrophysiol* 1991;14:1544–1553.
13. Bruce RA. Exercise testing of patients with coronary heart disease: principles and normal standards for evaluation. *Ann Clin Res* 1971;3:323–332.
14. Devereux R, Reichek N. Echocardiographic determination of left ventricular mass in man. *Circulation* 1977;613:613–618.
15. Merlet P, Valette H, Dubois RJ, et al. Prognostic value of cardiac metaiodobenzylguanidine imaging in patients with heart failure. *J Nucl Med* 1992;33:471–477.
16. Kurata C, Tawarahara K, Taguchi T, et al. Myocardial emission computed tomography with iodine-123-labeled beta-methyl-branched fatty acid in patients with hypertrophic cardiomyopathy. *J Nucl Med* 1992;33:6–13.
17. Horie H, Pamplin PJ, Yokota T. Inhibition of nociceptive neurons in the shell region of nucleus ventralis posterolateralis following conditioning stimulation of the periaqueductal grey of the cat. *Brain Res* 1991;561:35–42.
18. Jaques JS, Tobes MC, Sisson JC, Baker JA, Wieland DM. Comparison of the sodium dependency of uptake of MIBG and norepinephrine in cultured bovine adrenomedullary cells. *Mol Pharmacol* 1984;26:539–546.
19. Brown AM. Excitation of afferent cardiac sympathetic nerve fibers during myocardial ischemia. *J Physiol* 1967;190:35–53.
20. Uchida Y, Murao S. Excitation of afferent cardiac sympathetic nerve fibers during coronary occlusion. *Am J Physiol* 1974;226:1094–1099.
21. Thoren P. Activation of left ventricular receptors with nonmedullated vagal afferent fibers during occlusion of a coronary artery in the cat. *Am J Cardiol* 1976;37:1046–1051.
22. Muntz KH, Hagler HK, Boulas J, Willerson JT, Buja LM. Redistribution of catecholamines in the ischemic zone of the dog heart. *Am J Pathol* 1954;114:64–78.
23. Schwaiger M, Guibourg H, Rosenspire K, et al. Effect of regional myocardial ischemia on sympathetic nervous system assessed by fluorine-18-metaraminal. *J Nucl Med* 1991;31:1352–1357.
24. Miyazaki T, Zips DP. Presynaptic modulation of efferent sympathetic and vagal neurotransmission in the canine heart by hypoxia, high K+, low pH, and adenosine. *Circ Res* 1990;66:289–301.
25. Tsuchimochi S, Tamaki N, Shirakawa S, et al. Evaluation of myocardial distribution of iodine-123-labeled metaiodobenzylguanidine ([$^{123}$I]MIBG) in normal subjects. *Jpn J Nucl Med* 1994;31(3):257–264.
26. Maublant JC, Peycelon P, Kwiatkowski F, et al. Comparison between 180° and 360° data collection in technetium-99m-MIBI SPECT of the myocardium. *J Nucl Med* 1989;30:295–300.
27. Alman K, Steven MJ, Wieland DM, et al. Noninvasive assessment of cardiac diabetic neuropathy by carbon-11-hydroxyephedrine and position emission tomography. *J AM Coll Cardiol* 1993;22:1425–1432.
28. Gottlieb SO, Gottlieb SH, Achuff SC, et al. Silent ischemia on Holter monitoring predicts mortality in high-risk postinfarction patients. *JAMA* 1988;125:1030–1035.
29. Amsterdam EA. Relation of silent myocardial ischemia to ventricular arrhythmias and sudden death. *Am J Cardiol* 1988;62:241–271.
30. Sheps DS, Heiss G. Sudden death and silent myocardial ischemia. *Am Heart J* 1989;117:177–184.